Cr^{4+}-Doped $Y_3Al_5O_{12}$ as a Saturable Absorber for a Q-Switched and Mode-Locked 639-nm Pr^{3+}-Doped $LiYF_4$ Laser

2013 Appl. Phys. Express 6 032703

(http://iopscience.iop.org/1882-0786/6/3/032703)

Applied Physics Express **6** (2013) 032703
http://dx.doi.org/10.7567/APEX.6.032703

Cr^{4+}-Doped $Y_3Al_5O_{12}$ as a Saturable Absorber for a Q-Switched and Mode-Locked 639-nm Pr^{3+}-Doped $LiYF_4$ Laser

Ryo Abe, Junichiro Kojou, Kensuke Masuda, and Fumihiko Kannari*

Department of Electronics and Electrical Engineering, Keio University, Yokohama 223-8522, Japan
E-mail: kannari@elec.keio.ac.jp

Received December 29, 2012; accepted February 1, 2013; published online February 20, 2013

We experimentally prove that a Cr^{4+}-doped $Y_3Al_5O_{12}$ (YAG) crystal exhibits saturable absorption in visible wavelengths at 639, 607, and 521 nm. From *z*-scan measurements, the saturation energies measured using laser pulse widths of 25 and 66 ns at 639 nm are estimated to ~11.5 and 21.2 mJ/cm^2, respectively. Therefore, the absorption response time will be shorter than these pulse widths. Using the Cr^{4+}:YAG saturable absorber, we demonstrate for the first time, to the best of our knowledge, the passive Q-switched and the Q-switched mode-lock Pr^{3+}-doped $LiYF_4$ (YLF) lasers at 639 nm pumped by an InGaN diode laser.

The Cr^{4+}-doped $Y_3Al_5O_{12}$ (Cr^{4+}:YAG) crystal is a perfect saturable absorber to generate Q-switched and mode-locked pulses in the 1-μm-wavelength regime owing to its excellent optical, thermal, and mechanical properties. Passive Q-switched and mode-locked lasers down to 946 nm have been reported. The 1 μm absorption band is assigned to the $^3B_1(^3A_2) \rightarrow {}^3A_2(^3T_1)$ transition.[1] Cr^{4+}:YAG crystal also exhibits a strong absorption band at the red wavelength corresponding to the $^3B_1(^3A_2) \rightarrow {}^3E(^3T_1)$ transition.[1] However, since no intense laser pulse is available in the red color transitions, saturable absorption at the red color band remains unproved.

Trivalent praseodymium (Pr^{3+})-doped materials have proven to be very promising laser sources for efficient stimulated emission in the visible region.[2] Laser action (red at 720, 697, and 639 nm, orange at 607 nm, and green at 522 nm) has already been demonstrated with Pr^{3+}-doped fluoride crystals using InGaN diode lasers as a pumping laser source.[3–5] With advances in InGaN diode laser development, we can realize a high-power, compact all-solid-state laser that emits in the visible spectral region. In fact, Gün et al. have recently reported an output power of 938 mW at 639 nm with a maximum absorbed pump power of ~1.5 W using two InGaN laser diodes.[6] Pr^{3+}-doped fluoride glass fiber lasers have also been developed, and their wavelength tunability in the full visible wavelength region has been demonstrated.[7] Therefore, a passive Q-switch working in the visible wavelength region is strongly demanded.

In this letter, we report a *z*-scan measurement to examine the saturable absorption of a Cr^{4+}:YAG crystal at 639, 607, and 522 nm using active Q-switched Pr^{3+}-doped $LiYF_4$ (Pr^{3+}:YLF) laser pulses. We demonstrate for the first time that the Cr^{4+}:YAG crystal can be used as a Q-switch in Pr^{3+}:YLF lasers at 639 nm. Moreover, Q-switched mode-locking is also demonstrated.

The diameter of the Cr^{4+}:YAG crystal (fabricated by Scientific Materials Inc.) used in our experiments was 4 mm, and it was 1.3 mm thick. Antireflection coating, which is effective for 600–640 nm, was performed by the crystal manufacturer. The initial transmittance of our crystal at low fluences was, thus, 88.5% at 633 nm. The laser source was an active Q-switched Pr^{3+}:YLF laser.[8] The highest incident laser energies delivered by the laser pulse at wavelengths of 639, 607, and 522 nm with pulse widths (FWHM) of 26, 25, and 130 ns were 3.6, 1.3, and 0.41 μJ, respectively. The time history of the 639-nm laser pulse is shown in Fig. 1. The

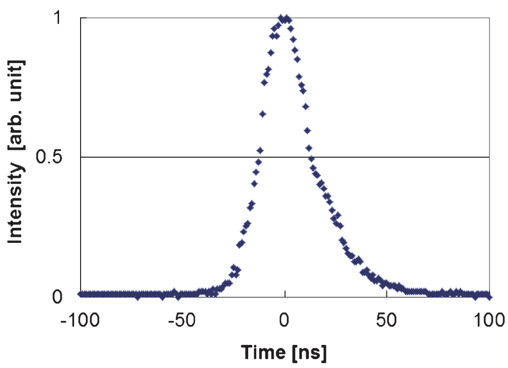

Fig. 1. Time history of a 639-nm laser pulse used for *z*-scanning measurement of a Cr^{4+}:YAG.

pulse repetition rate was 11 kHz. The laser energy launched to the Cr^{4+}:YAG crystal was adjusted using a neutral-density filter. The laser beam was focused by a spherical lens with a focus length of $f = 75$ mm. We measured the change in the beam spot size along the optical axis in air using a beam profiler. The laser spot was in a Gaussian shape with a diameter at the focal point of 10.2 μm at 639 nm. The estimated M^2 of the laser was ~2.5. Then, the spot size in the Cr^{4+}:YAG crystal ($n = 1.83$) was calculated using ABCD matrices. We adjusted the highest incident laser energy so that almost 100% transmission was obtained when the crystal was placed at the focus. The laser fluence at the crystal's center when the 1.3-mm-thick Cr^{4+}:YAG crystal was placed so that its center corresponds to the focal point of the focusing lens in the air was estimated as 93, 37, and 16 mJ/cm^2 for 639, 607, and 522 nm, respectively. On a translation stage, the crystal was moved parallel to the laser beam axis with 10 μm precision.

Z-scan measurements were plotted, as shown in Fig. 2. Clear saturation in the absorption was observed at three wavelengths. At 639 nm, we performed more detailed *z*-scan measurements using a pulsed laser with pulse widths of 66 or 25 ns. The laser pulse width was adjusted by changing the pumping power of the actively Q-switched Pr^{3+}:YLF laser.[8] The beam profile did not change at pulse length change. The laser fluences that reduce the absorption coefficient to half of the initial value were 21.2 and 11.5 mJ/cm^2 for pulse widths of 66 and 25 ns, respectively, as shown in Fig. 3. At a 1 μm wavelength, ground-state absorption cross sections σ of Cr^{4+}:YAG reportedly vary by more than one order of magnitude from 3.6×10^{-19} to 5×10^{-18} cm^2.[9] Thus, the corre-

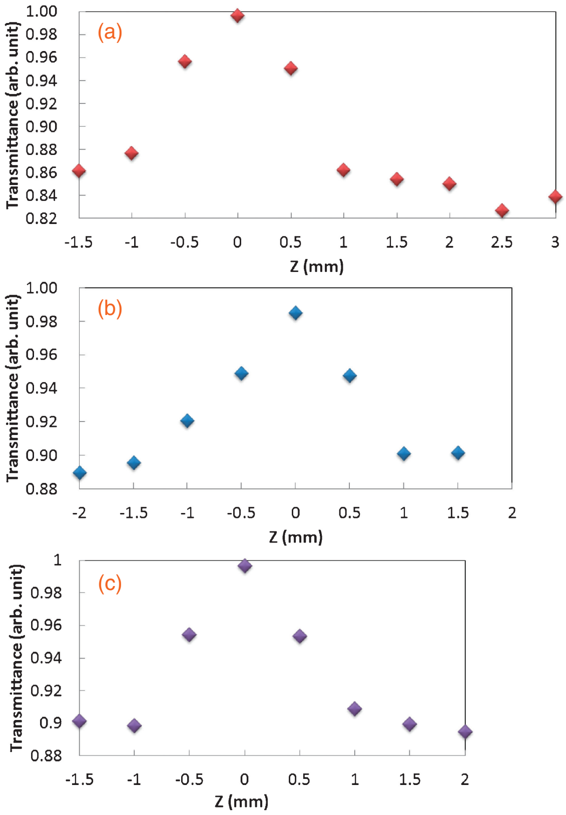

Fig. 2. Plots of normalized transmittance of a Cr^{4+}:YAG crystal as a function of crystal center position in z-scan measurement: λ = (a) 639 nm, (b) 607 nm, and (c) 522 nm. $z = 0$ corresponds to focal point of focusing lens ($f = 75$ mm) in the crystal.

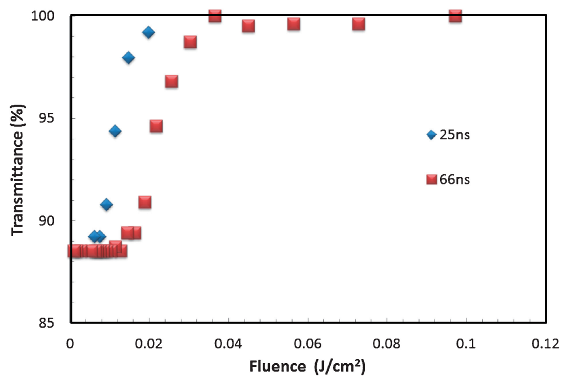

Fig. 3. Plots of transmittance of a Cr^{4+}:YAG crystal as a function of laser fluence at crystal center in z-scan measurement. Laser pulse widths are 25 and 66 ns for triangle and circle plots, respectively.

sponding saturation fluence $h\nu/\sigma$ is in the range of 40–550 mJ/cm^2. Since the absorption coefficient at 639 nm is larger than that at 1 µm,[1] it will be reasonable that we obtained smaller saturation fluences at 639 nm. Since the saturation energy estimated for the Cr^{4+}:YAG in our measurements increases by a factor of ~2 when the laser pulse width increases from 25 to 66 ns, the absorption saturation is defined using the intensity rather than the fluence in this pulse width regime. In other words, the response time of the ground-state absorption will be at least shorter than 25 ns, which is much shorter than the response time at the 1 µm wavelength of 3.5 µs.[10] Presumably, by phonon moderated processes, $^3E(^3T_1)$ level quickly decays to lower states. The response

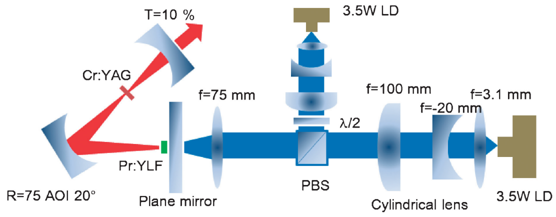

Fig. 4. Schematic of experimental setup of passive Q-switch and Q-switched mode-lock Pr^{3+}:YLF laser.

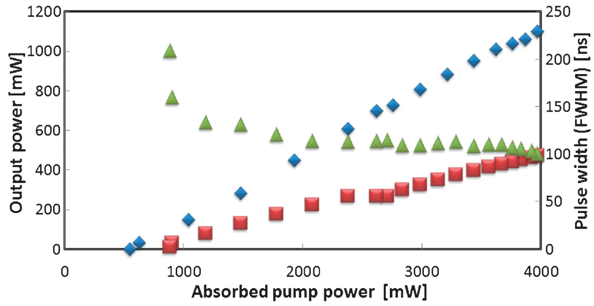

Fig. 5. Plots of Q-switched laser performance as a function of absorbed pump power: averaged output power (square); and pulse width of Q-switched pulse envelope (triangle). Diamond plots show cw output laser power obtained without Cr^{4+}:YAG crystal.

time may correspond to the effective lifetime of those mid-states. The detail of the energy diagram and dynamic in Cr^{4+}:YAG crystals needs further investigation based on experiments such as direct recovery time measurement for the ground-state absorption and detailed analysis including contribution of excited state absorption.[9]

In our passive Q-switching experiment, we employed a V-shaped cavity with two laser mode waists (Fig. 4) and pumped a 3.7-mm-long Pr^{3+}:YLF crystal (Pr^{3+} 0.5 at. %) with two 3.5 W InGaN diode lasers (Nichia) emitting around 444 nm, which were combined with a polarization beam splitter (PBS). The flat mirror is highly reflective (HR) coated (>99.7%) at 639 nm and antireflective coated at 444 nm. The folding mirror with a 75 mm curvature radius is HR coated (>99.7%) at 639 nm. The angle of incidence was designed as 20°. The output coupler with a 75 mm curvature radius has a transmission of 10% at 639 nm. The beam waist diameters of the fundamental cavity mode were ~28 × 66 and ~41 × 92 µm^2 in the Pr^{3+}:YLF and Cr^{4+}:YAG crystals, respectively, for a cavity length of 225 mm. The pump beam waist diameter was 6.6 × 14 µm^2 in the laser crystal. We calculated the mode matching efficiency by spatially integrating the mode overlapping factor for our setup as $\eta_m \sim 75.5\%$. The Cr^{4+}:YAG crystal used in the z-scan measurements, with an initial transmission of 88.5%, was used as the saturable absorber.

Figure 5 shows plots of the average output power of the Q-switched laser at 639 nm as a function of absorbed pump power. Changes in the pulse width (envelope of Q-switched pulse) are also plotted. The highest laser power of 475 mW was obtained at an absorbed pump power of 4 W with a slope efficiency of ~15%. The repetition rate of Q-switching is 120 kHz. The repetition rate monotonically increased as the pump power increases. We obtained the highest cw output power of 1.1 W at a pump power of 4 W with a slope efficiency of ~33% using the same V-shaped cavity without

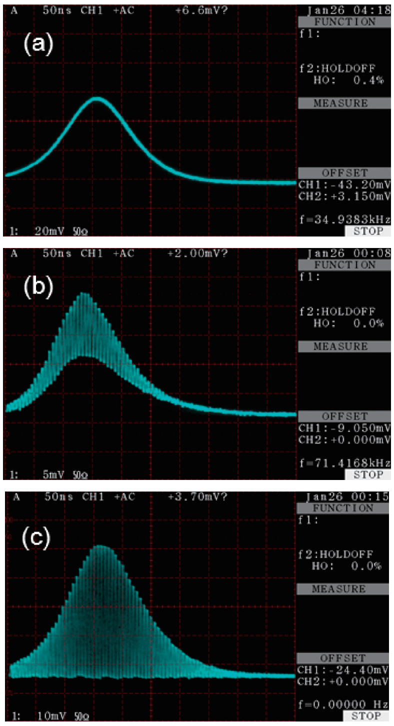

Fig. 6. Evolution of Q-switched mode-lock laser oscillation with increase of pump power. Time histories of laser pulse at absorbed pump powers of (a) 1.3, (b) 2, and (c) 4 W, respectively. These time histories were measured with a photodiode (300 MHz) and an analog oscilloscope (1 GHz).

the Cr^{4+}:YAG crystal. When slightly displacing the position of the Cr^{4+}:YAG crystal from the confocal position of the two concave mirrors, the laser power monotonically decreases and the pulse width gradually increases. Q-switched mode-locking started when the absorbed pump power reached ~2.2 W. Figure 6 shows time histories of Q-switch and Q-switched mode-lock laser pulses obtained at an absorbed pump power of 1.3, 2, and 4 W, respectively. These time histories were measured with a photodiode (300 MHz) and an analog oscilloscope (1 GHz). The Q-switched mode-lock laser pulse was also measured with a fast photodiode (40 GHz) and an analogue oscilloscope (1 GHz). A 100% modulation depth was obtained at an absorbed pump power of 4 W. The pulse repetition rate of the mode-locked pulse is 667 MHz as shown in Fig. 7, which corresponds to the cavity round-trip length of 45 cm. The laser spectrum was slightly broadened to 0.32 nm at mode-locking from the cw laser.

From our observation of Q-switched mode-locking, it is still not clear which transition in Cr^{4+} is responsible to this fast modulation. At wavelength of 1 μm, although the similar Q-switched mode-locking has been observed using Cr^{4+}:YAG saturable absorbers, no cw mode-locking has been realized since the fast modulation is caused by excited state absorption. The lifetime of the second excited state of Cr^{4+}:YAG at 1 μm was estimated to ~0.1 ns.[11] Although our z-scan measurement predicted shorter absorption recovery times for the ground-state absorption, if the similar excited state absorption is involved also in the Q-switched mode-locking of Pr^{3+}:YLF lasers, it is difficult to achieve cw mode-locking at 639 nm with Cr^{4+}:YAG.

We compared a cadmium selenium sulfide ($CdSe_{1-x}S_x$) colloidally colored glass, which had been previously used as

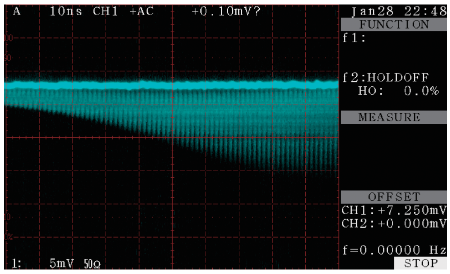

Fig. 7. Enlarged time history of Q-switched mode-lock laser pulses (reversed) measured with a fast photodiode (40 GHz) at an absorbed pump power of 4 W.

a saturable absorber to demonstrate the initiation of Kerr-lens mode-locking in picosecond Pr^{3+}:YLF lasers.[12] The thickness of the colored glass filter (Schott Glass RG610) was reduced to 90 μm, at which the initial transmission at 639 nm was ~99.3%. The glass plate was inserted at a Brewster angle into the same V-shaped cavity. The shortest Q-switch pulse width obtained with this glass filter was 790 ns (FWHM) at a pulse repetition rate of 256 kHz at an absorbed pump laser power of 4 W. The pulse exhibited Q-switched mode-locking with a modulation depth of ~45%. Presumably, the poor laser output performance compared with that obtained with the Cr^{4+}:YAG crystal is caused by higher saturation fluence than that of the Cr^{4+}:YAG crystal. On the other hand, since the absorption of the colored glass filter is caused by the quantum confinement nature of the semiconductor microcrystallities in the glass, the absorption recovery time is much faster (<100 ps). Therefore, as already demonstrated using Ar-ion laser pumping,[12] thin colored glass filter is a promising candidate to establish an all-solid-state cw mode-lock laser at 639 nm using Pr^{3+}:YLF crystals.

In conclusion, to the best of our knowledge, we reported the first passively Q-switched and the Q-switched mode-lock lasers using a Cr^{4+}:YAG saturable absorber in the visible range at 639 nm. Since we also proved saturable absorption at 522 nm in our experiment, short pulse generation in the green transition might also be possible.

Acknowledgment This research was supported by a Grant-in-Aid from the Ministry of Education, Culture, Sports, Science and Technology, Japan for the Photon Frontier Network Program.

1) R. Feldman, Y. Shimony, and Z. Burshtein: Opt. Mater. **24** (2003) 333.
2) T. Sandrock, T. Danger, E. Heumann, G. Huber, and B. H. T. Chai: Appl. Phys. B **58** (1994) 149.
3) A. Richter, E. Heumann, E. Osiac, G. Huber, W. Seelert, and A. Diening: Opt. Lett. **29** (2004) 2638.
4) K. Hashimoto and F. Kannari: Opt. Lett. **32** (2007) 2493.
5) N. O. Hansen, A. R. Bellancourt, U. Weichmann, and G. Huber: Appl. Opt. **49** (2010) 3864.
6) T. Gün, P. Metz, and G. Huber: Opt. Lett. **36** (2011) 1002.
7) H. Okamoto, K. Kasuga, I. Hara, and Y. Kubota: Opt. Express **17** (2009) 20227.
8) J. Kojou, Y. Watanabe, Y. Kojima, H. Nemoto, and F. Kannari: Appl. Opt. **51** (2012) 1382.
9) G. Xiao, J. H. Lim, S. Yang, E. V. Stryland, M. Bass, and L. Weichman: IEEE J. Quantum Electron. **35** (1999) 1086.
10) A. G. Okhrimchuk and A. V. Shestakov: Phys. Rev. B **61** (2000) 988.
11) S. Wang, Q. Li, S. Du, Q. Zhang, Y. Shi, J. Xing, D. Zhang, B. Feng, Z. Zhang, and S. Zhang: Opt. Commun. **277** (2007) 133.
12) S. Ruan, J. M. Sutherland, P. M. W. French, J. R. Taylor, and B. H. T. Chai: Opt. Lett. **20** (1995) 1041.